MICROSTRUCTURE OF A RAPIDLY QUENCHED NANOCRYSTALLINE $Hf_{11}Ni_{89}$ ALLOY FROM X-RAY DIFFRACTION

J. Gubicza, G. Ribárik, I. Bakonyi[*] and T. Ungár

Department of General Physics, Eötvös University, P.O.Box 32, H-1518, Budapest, Hungary
[*]Research Institute for Solid State Physics and Optics, Hungarian Academy of Sciences, P.O.Box 49, H-1525 Budapest, Hungary

Abstract

A rapidly quenched nanocrystalline $Hf_{11}Ni_{89}$ alloy was produced by melt-spinning. The X-ray phase analysis shows that the as-quenched ribbon consists of mainly nanocrystalline fcc $HfNi_5$ although a small amount of Ni is also detected. The crystallite size distribution and the dislocation structure of the dominant $HfNi_5$ phase were determined by a recently developed method of diffraction profile analysis. In this procedure, by assuming spherical shape and log-normal size distribution of crystallites, the measured physical intensity profiles are fitted by the well established *ab initio* functions of size and strain peak profiles. The anisotropic broadening of peak profiles is accounted for by the dislocation model of the mean square strain in terms of average dislocation contrast factors. It was found that the median and the variance of the crystallite size distribution are 3.3 nm and 0.70, respectively. The dislocation density is 5.7×10^{16} m^{-2} and the character of dislocations is nearly pure screw.

Keywords: crystallite size, size distribution, dislocations, nanocrystalline $HfNi_5$, X-ray peak profile analysis, anisotropic peak broadening.

1. INTRODUCTION

X-ray diffraction (XRD) is an effective tool for the determination of microstructure of nanocrystalline materials. X-ray diffraction line profiles are broadened due to the smallness of crystallites and the lattice distortions. The two effects can be separated on the basis of the different diffraction order dependence of peak broadening. The standard methods of X-ray diffraction profile analysis based on the full widths at half maximum (FWHM), the integral breadths and on the Fourier coefficients of the profiles provide the apparent crystallite size and the mean square strain [1-3]. At the same time, it has been shown in several works (see, e.g., Ref. 4) that the shape of the diffraction profiles depends not only on the mean size but also on the size-distribution and the shape of crystallites. If the shape of the crystallites can be assumed to be uniform, the area- and the volume-weighted mean crystallite sizes can be determined from the Fourier cefficients and the integral breadths of the X-ray diffraction profiles [4-8]. These two mean sizes of crystallites can be used for the determination of a crystallite size distribution function having two free parameters [4,5,8,9]. The evaluation of the X-ray profiles is further complicated by the anisotropic strain broadening of the diffraction lines. This means that neither the full width at half maximum nor the integral breadth nor the Fourier coefficients of the profiles are monotonous functions of the diffraction vector [10-12]. It has been shown recently that the strain anisotropy can be well accounted for by the dislocation model of the mean square strain by introducing the contrast factors of dislocations [13-18]. Since the values of the dislocation contrast factors depend on the type of dislocations present in the crystal, the evaluation of X-ray profiles for the contrast factors enables the determination of the dislocation structure.

An evaluation procedure of X-ray diffraction profiles was elaborated recently for the determination of crystallite size distribution and the dislocation structure in nanocrystalline materials [19]. In this method the measured physical profiles are fitted by the well established *ab initio* functions of size and strain peak profiles. Assuming spherical crystallite shape and log-normal size distribution, the Fourier transform of the size profile has been derived in a relatively simple closed form. The inverse Fourier transform of this formula gives the theoretical size intensity profile. Strain is assumed to be caused by dislocations and the strain part of the peak broadening is modelled by the mean square strain in dislocated crystal as derived by Wilkens [15]. The fitting procedure is carried out by the method of least squares where the only fitting parameters are the median and the variance of the size distribution of crystallites, the density and the arrangement parameter of dislocations and one parameter for the dislocation contrast factors. This novel XRD procedure has been applied for the microstructural characterization of a nanocrystalline $Hf_{11}Ni_{89}$ alloy ribbon produced in a single step by rapid solidification [20,21]. The structure of this ribbon has been previously studied by conventional and high-resolution transmission electron microscopy (TEM) [21-23], and XRD [22,23]. Even the high-resolution TEM study [23] indicated that the as-quenched ribbon contains a nanocrystalline $HfNi_5$ intermetallic compound phase only. However, the presence of a small amount of a ferromagnetic phase could be identified by magnetic measurements [23,24] which was ascribed to a Ni(Hf) solid solution interfacial phase due to a Ni-enrichment of the grain boundaries. In the present work, the crystallite size distribution and the dislocation structure of the $HfNi_5$ phase have been determined by the recently developed method of X-ray diffraction profile analysis in which the measured profiles are fitted by *ab initio* theoretical functions [19]. The lattice parameters of $HfNi_5$ and the interfacial phase are also presented.

2. EVALUATION OF THE X-RAY DIFFRACTION PROFILES

According to the kinematical theory of X-ray diffraction, the physical profile of a Bragg reflection is given by the convolution of the size and the distortion profiles [3]

$$I^P = I^S * I^D \;, \tag{1}$$

where the superscripts *S* and *D* stand for size and distortion, respectively. The Fourier transform of this equation gives [3]

$$A(L) = A^S(L)\, A^D(L), \tag{2}$$

where $A(L)$ are the absolute values of the Fourier coefficients of the physical profiles, A^S and A^D are the size and the distortion Fourier coefficients and L is the Fourier variable.

Assuming that in the crystal the lattice distortions are caused by dislocations, the Fourier coefficients of the strain profile can be given as [3,13-15]

$$A^D_g\,(\mathrm{L}) = \exp[-\,\rho \mathrm{B} \mathrm{L}^2 f(\eta)\, K^2 \overline{C}]\;, \tag{3}$$

where $\mathrm{B}=\pi \mathrm{b}^2/2$, $\eta \sim L/R_e$, R_e is the effective outer cut-off radius of dislocations and $f(\eta)$ is a function derived explicitely by Wilkens [15]. The explicite form of $f(\eta)$ can be found in equations A.6 to A.8 in Ref. 15. The asymptotic behaviour of $f(\eta)$ is:

$$f(\eta) \sim -\ln\eta \;, \quad \text{if } \eta \leq 1 \tag{4}$$

and

$$f(\eta) \sim \frac{1}{\eta}\;, \qquad \text{if } \eta \geq 1 \;. \tag{5}$$

Instead of $\mathrm{R_e}$, it is physically more appropriate to use the dimensionless parameter $M = \mathrm{R_e}\sqrt{\rho}$ defined by Wilkens as the dislocation arrangement parameter [15]. The value of M gives the strength of the dipole character of dislocations: the higher the value of M, the weaker the dipole character and the screening of the displacement fields of dislocations [15].

The average dislocation contrast factors are the weighted average of the individual C factors either over the dislocation population or over the permutations of the *hkl* indices [25-27]. Based on the theory of line broadening caused by dislocations, it can been shown that in an untextured cubic polycrystalline specimen the values of $\overline{C}$ are simple functions of the invariants of the fourth order polynomials of *hkl* [27]

$$\overline{C} = \overline{C}_{h00}\,[1 - q(h^2k^2 + h^2l^2 + k^2l^2)/(h^2+k^2+l^2)^2], \tag{6}$$

where $\overline{C}_{h00}$ is the average dislocation contrast factor for the *h00* reflections, q is a parameter depending on the elastic constants and on the character of dislocations (e.g. edge or screw type) in the crystal.

It was observed by many authors that in powder or bulk nanocrystalline specimens the crystallite-size distribution density can be described by log-normal function [4,8,9,28]

$$f(x)=\frac{1}{\sqrt{2\pi}\,\sigma}\frac{1}{x}\exp\left\{-\frac{[\ln(x/m)]^2}{2\sigma^2}\right\}, \quad (7)$$

where x is the crystallite size, σ^2 is the lognormal variance and m is the median of the size distribution density function, $f(x)$. For spherical crystallites with log-normal size distribution, the area-, volume- and arithmetically weighted mean crystallite sizes are obtained as [4]

$$\langle x\rangle_{area}=m\cdot\exp(2.5\cdot\sigma^2). \quad (8)$$

$$\langle x\rangle_{vol}=m\cdot\exp(3.5\cdot\sigma^2). \quad (9)$$

$$\langle x\rangle_{arithm}=m\cdot\exp(0.5\cdot\sigma^2). \quad (10)$$

Assuming spherical crystallite shape with log-normal size distribution, the Fourier transform of the size profile can be given as:

$$A^S(L)\sim\frac{m^3\exp(4.5\sigma^2)}{3}erfc\left[\frac{\ln(|L|/m)}{\sqrt{2}\,\sigma}-1.5\sqrt{2}\sigma\right]-$$
$$-\frac{m^2\exp(2\sigma^2)|L|}{2}erfc\left[\frac{\ln(|L|/m)}{\sqrt{2}\,\sigma}-\sqrt{2}\sigma\right]+\frac{|L|^3}{6}erfc\left[\frac{\ln(|L|/m)}{\sqrt{2}\,\sigma}\right]. \quad (11)$$

where *erfc* is the complementary error function.

A numerical procedure has been worked out for fitting the experimental profiles by the inverse Fourier transform of the product of the theoretical functions of size and strain Fourier transforms given in equations (3) and (11) [19]. The method has the following steps: (i) the theoretical Fourier coefficients of the size and strain profiles were determined by using eqs. (3-5) and (11), (ii) the theoretical intensity profiles were calculated by the inverse Fourier transformation of the theoretical Fourier coefficients, (iii) the experimental and the calculated intensity profiles were compared by the least squares method. The procedure has five fitting parameters for cubic crystals: (i) m and (ii) σ of the log-normal size distribution density function (assuming spherical crystallites), (iii) ρ and (iv) M in the strain profile and (v) q for the average dislocation contrast factors. Further details of the fitting procedure are given elsewhere [19].

3. EXPERIMENTAL

A $Hf_{11}Ni_{89}$ master alloy was melted and quenched into a ribbon (3 mm wide, 11 μm thick) by means of the melt-spinning technique. The process and its parameters have been described in detail elsewhere [20]. The diffraction profiles were measured in a Philips X'pert diffractometer using Cu anode and pyrolitic graphite secondary monochromator. The lattice parameters of the detected phases were determined from the positions of the diffraction peaks by extrapolating to $\theta=90^0$. The details of the profiles were measured in a special double-crystal, high-resolution diffractometer with negligible instrumental broadening. The overlapping peaks were better separated in these measurements due to the absence of the Kα doublet. A fine focus rotating cobalt anode (Nonius FR 591) was operated as a line focus at 36 kV and 50 mA (λ=0.1789 nm). The symmetrical 220 reflection of a Ge monochromator was used in order to have wavelength compensation at the

position of the detector. The $K\alpha_2$ component of the Co radiation was eliminated by an 0.16 mm slit between the source and the Ge crystal. The profiles were registered by a linear position sensitive gas flow detector, OED 50 Braun, Munich. In order to avoid air scattering and absorption, the distance between the specimen and the detector was overbridged by an evacuated tube closed by mylar windows.

In the present case, a strong overlap of the diffraction profiles has been observed. The overlapping peaks have been separated since the present evaluation method is worked out for individual profiles. Background subtraction and the separation of overlapping peaks are carried out in one step. Two or more analytical functions, usually of PearsonVII or Pseudo-Voigt type plus a linear background are fitted to the overlapping peaks. In the next step, the unwanted fitted peaks together with the linear background are subtracted leaving the targeted peak free of overlap and background. The procedure is then repeated for the other peaks. The separated profiles are taken as individual diffraction profiles in the evaluation procedures. It is noted here that the fitting of the PearsonVII or Pseudo-Voigt functions is only used for the separation of the overlapping peaks and subtraction of the background. The evaluation procedure is carried out on the measured profiles after separation using the inverse Fourier transform of the *ab-initio* functions of the size and strain Fourier coefficients, as described above. Due to the nanometer size of crystallites in $HfNi_5$ phase, the physical peak broadening is about two orders of magnitude larger than the instrumental effects of the Nonius diffractometer. Consequently, no instrumental corrections were necessary to be carried out.

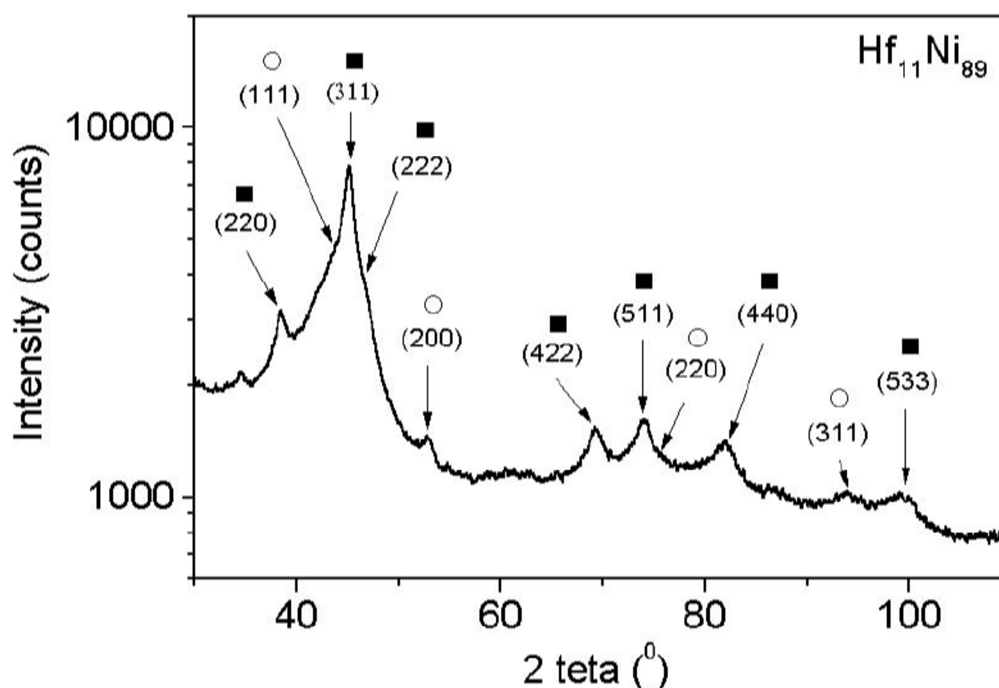

Fig. 1: The X-ray diffractogram of the as-quenched $Hf_{11}Ni_{89}$ alloy. Note that the intensity is in logarithmic scale. The solid squares and the open circles represent the $HfNi_5$ and the Ni phases, respectively.

4. RESULTS AND DISCUSSION

The X-ray diffractogram of the as-quenched $Hf_{11}Ni_{89}$ alloy is shown in Figure 1. Note that the intensity is scaled logarithmically in order to show the details of the peaks with lower intensities. The dominant crystalline phase is $HfNi_5$ which is consistent with the previous experiments on this

material [21-24]. The lattice parameter of this fcc phase is 0.6656±0.0003 nm which is smaller than the known parameter for the equilibrium $HfNi_5$ phase (0.6683 nm). This result is consistent with previous works [21,22] and it can be explained by the fact that the composition of the $Hf_{11}Ni_{89}$ alloy is far from the stoichiometry of the $HfNi_5$ intermetallic compound. A part of the excess Ni atoms can occupy the sites of the larger Hf atoms causing a decrease of the lattice parameter. The contraction of the lattice can also be caused by the nanocrystalline state of $HfNi_5$. A Ni phase with the lattice parameter 0.3517±0.0003 nm was also detected by X-rays which has been observed only by magnetic measurements on this material previously [23,24]. It can be seen from the diffractogram that the diffraction peaks are broadened due to the nanometer sized crystallites. As a consequence of this broadening, the profiles are overlapping. For analysing the diffraction peak profiles, the groups of peaks of the $HfNi_5$ phase were also measured by the double crystal diffractometer because of the negligible instrumental broadening of this device and the absence of the cobalt K alpha doublet. The background subtraction and the separation of the overlapping peaks were carried out by the procedure described in paragraph 3. The four most intensive reflections of the $HfNi_5$ phase (311, 422, 440, 533) were fitted by the theoretical functions of the size and strain profiles. The measured profiles and the fitted *ab initio* functions normalized to unity are shown in Figure 2. The correlation between the measured and fitted profiles is very good. The median, m, and the variance, σ, of the log-normal crystallite size distribution are 3.3 nm and 0.70, respectively. The crystallite size distribution function is plotted in Figure 3. According to equations (8-10), the arithmetic, the area-, and the volume-weighted mean crystallite sizes are 4.2, 11.2 and 18.3 nm, respectively, and are indicated in Figure 3. The results obtained from X-rays are in good agreement with previous transmission electron microscopy (TEM) observations [21,23].

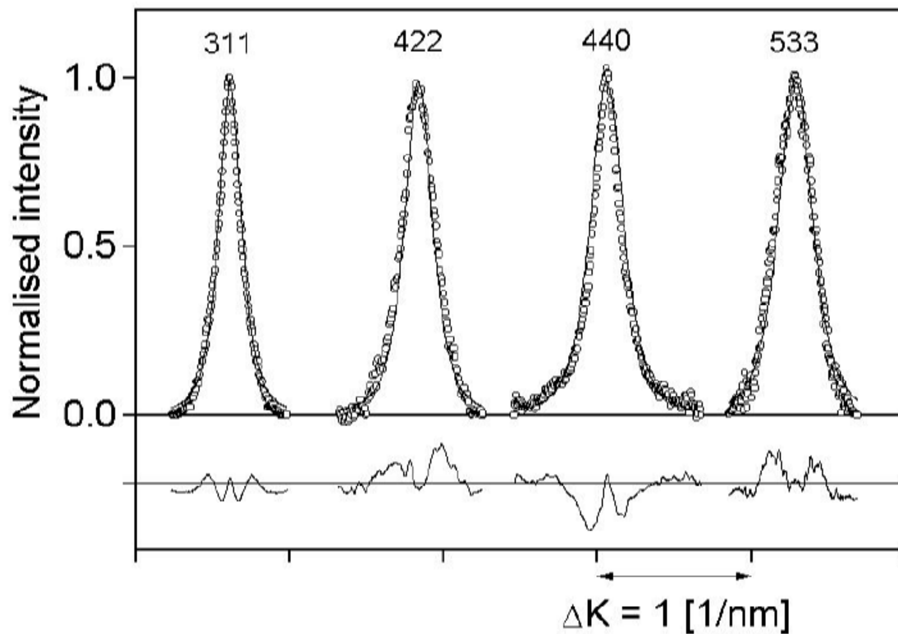

Fig. 2: The measured (open circles) and the fitted theoretical (solid line) intensity profiles for $HfNi_5$ phase. The differences between the measured and fitted values are also shown in the lower part of the figure. The indices of the reflections are also indicated.

The parameter q in the contrast factors of dislocations is 2.39±0.03. In a previous work, the values of q have been calculated for nickel using the elastic constants given by Hearmon [29] and assuming the most common dislocation slip system with the Burgers vector **b**=a/2<110>{111} [26]. It was found that for pure screw or pure edge dislocations the values of q are 2.23 or 1.38, respectively.

The experimental value of q obtained for $HfNi_5$ is compared to these values since to the best knowledge of the authors, the anisotropic elastic constants of $HfNi_5$ are not available. The experimental value of q is much closer to the value corresponding to screw dislocations in Ni, however, it is, well beyond experimental error, out of the permitted range for edge and screw dislocations. The discrepancy can originate from the difference between the elastic constants of $HfNi_5$ and Ni, or it can be resolved by finding a type of dislocation which is still compatible with the fcc lattice but provides a larger range for the values of q. In a previous paper, it was shown that the <111>{110} type dislocations yield a higher range for the q values at the same elastic constants: q=2.63 and 1.37 for pure screw and edge dislocations in Ni, respectively [26]. The <111>{110} type dislocations in an fcc lattice are in prismatic loops observed with a considerable density in the TEM micrographs of heat-treated nanocrystalline nickel [30]. Nevertheless, we can conclude that the character of the prevailing dislocations in $HfNi_5$ is nearly pure screw. For these conditions: $\bar{C}_{h00}$=0.266±0.01 [26]. This value and the length of the Burgers vector (b=a/$\sqrt{2}$) were used as input parameters in the fitting of the Fourier coefficients. The dislocation density is obtained to be $\rho=5.7\times10^{16}$ m^{-2}. The average distance between the dislocations is $\rho^{-0.5}$=5.2 nm which means that each crystallite contains only a few dislocations on the average.

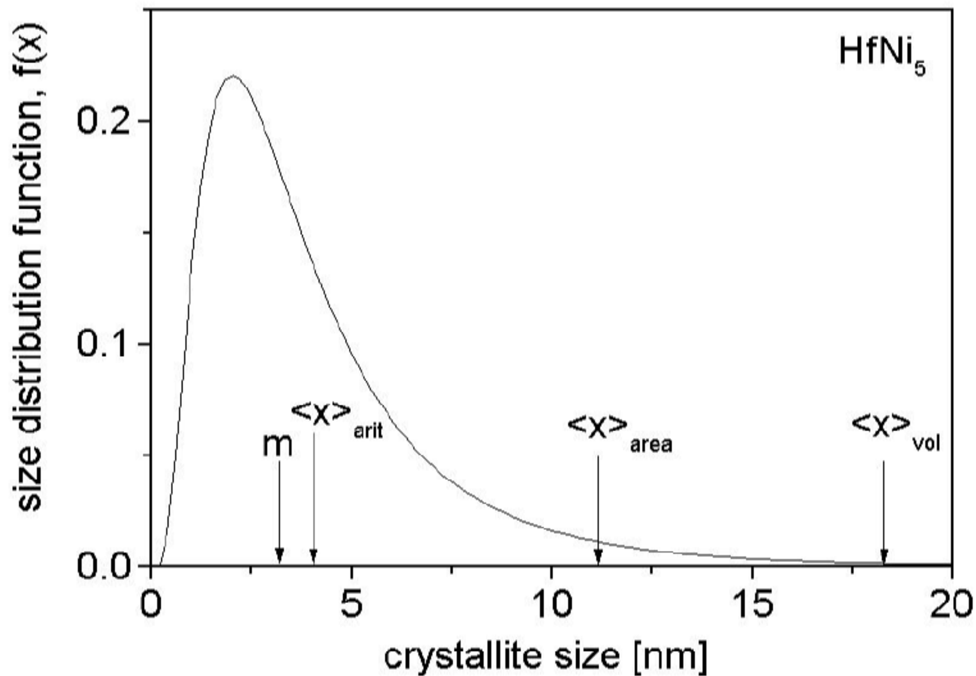

Fig. 3: The crystallite-size distribution function, f(x), for $HfNi_5$ phase determined by X-rays. The median, m, of the size distribution, the arithmetical, $\langle x\rangle_{arit}$, the area-, $\langle x\rangle_{area}$, and the volume-, $\langle x\rangle_{vol}$, weighted mean crystallite sizes are also indicated.

5. CONCLUSIONS

The crystallite size distribution and the dislocation structure in nanocrystalline $HfNi_5$ were determined by X-ray diffraction peak profile analysis. The median and the variance of the crystallite size distribution were found to be 3.3 nm and 0.70, respectively. This means that the size of the crystallites are in nanometer scale with wide distribution which are in good correlation with previous TEM results. The difference between the values of the measured dislocation contrast factors and those calculated for the most common fcc dislocation slip system, <110>{111}, was

explained by the existence of the <111>{110} type bcc dislocations in prismatic loops. It was concluded that the character of the prevailing dislocations in $HfNi_5$ is nearly pure screw. The average dislocation density is found to be $5.7x10^{16}$ m^{-2}.

ACKNOWLEDGEMENTS

The authors are grateful for the financial support of the Hungarian Scientific Research Fund, OTKA, Grant Nos. T031786, T022124 and D-29339.

REFERENCES

1. G. K. Williamson and W. H. Hall, Acta Metall. 1, (1953), p.22.
2. B. E. Warren and B. L. Averbach, J. Appl. Phys. 21, (1950), p.595.
3. B. E. Warren, Progr. Metal Phys. 8**,** (1959), p.147.
4. J. I. Langford, D. Louer and P. Scardi, J. Appl. Cryst. 33 (2000), p.964.
5. C. E. Krill and R. Birringer, Phil. Mag. A 77**,** (1998), 621.
6. M. Rand, J. I. Langford and J. S. Abell, Phil. Mag. B 68**,** (1993), p.17.
7. A. J. C. Wilson, X-ray Optics, Methuen, London. (1962), p.1.
8. J. Gubicza, J. Szépvölgyi, I. Mohai, L. Zsoldos and T. Ungár, Mat. Sci. Eng. A 280, (2000), p.263.
9. Ch. D. Terwilliger and Y. M. Chiang, Acta Met. Mater. 43**,** (1995), p.319.
10. G. Caglioti, A. Paoletti and F. P. Ricci, Nucl. Instrum. 3, (1958), p.223.
11. P. Suortti, in The Rietveld Method, edited by R. A. Young, IUCr Monographs on Crystallography, Vol. 5., Oxford University Press, (1993), p.167.
12. A. Le Bail, Proc. Accuracy in Powder Diffraction II, NIST Special Publication, 846, (1992) p.142.
13. M. A. Krivoglaz, Theory of X-ray and Thermal Neutron Scattering by Real Crystals, Plenum Press, N. Y. (1996) and X-ray and Neutron Diffraction in Nonideal Crystals, Springer-Verlag, Berlin Heidelberg New York. (1969), p.1.
14. M. Wilkens, phys. stat. sol. (a) 2, (1970), p.359.
15. M. Wilkens, Fundamental Aspects of Dislocation Theory, ed. J. A. Simmons, R. de it, R. Bullough, Vol. II. Nat. Bur. Stand. (US) Spec. Publ. No. 317, Washington, DC. USA, (1970), p. 1195.
16. P. Klimanek and Jr R. Kuzel, J. Appl. Cryst. 21**,** (1988), p.59.
17. T. Ungár and A. Borbély, Appl. Phys. Lett. 69 (1996), p.3173.
18. P. Scardi and M. Leoni, J. Appl. Cryst. 32**,** (1999), p.671.
19. T. Ungár, J. Gubicza, G. Ribárik and A. Borbély, J. Appl. Cryst. (2001), in the press.
20. I. Bakonyi, F. Mehner, M. Rapp, A. Cziráki, H. Kronmüller and R. Kirchheim, Z. Metallkd. 86, (1995), p.619.
21. I. Bakonyi and Á. Cziráki, Nanostruct. Mater. 11, (1999), p.9.
22. K. Lu, Z.F. Dong, I. Bakonyi and Á. Cziráki, Acta Metall. Mater. 43, (1995), p.2641.
23. R. Lück, Z. F. Dong, M. Scheffer, I. Bakonyi and K. Lu, Phil. Mag. B, 79, (1999), p.163.
24. Z. F. Dong, K. Lu, R. Lück, I. Bakonyi and Z.Q. Hu, Nanostruct. Mater. 9, (1997), p.363.
25. R. Kuzel and P. Klimanek, J. Appl. Cryst. 21**,** (1988), p.363.
26. T. Ungár, I. Dragomir, Á. Révész and A. Borbély, J. Appl. Cryst. 32**,** (1999), p.992.
27. T. Ungár and G. Tichy, phys. stat. sol. (a) 171**,** (1999), p.425.
28. T. Ungár, A. Borbély, G. R. Goren-Muginstein, S.Berger and A. R. Rosen, Nanostructured Materials 11**,** (1999), p.103.
29. R. F. S. Hearmon, in *Landolt-Börnstein*, **1**, (1966), p.1.
30. Á. Cziráki, Zs. Tonkovics, L. Gerőcs, B. Fogarassy, I. Groma, E. Tóth-Kádár, T. Tarnóczi and I. Bakonyi,. Mater. Sci. Eng., A179/A180, (1994), p.531.